Inorganic Chemistry

Article

pubs.acs.org/IC

Structural Effects Behind the Low Temperature Nonconventional Relaxor Behavior of the $Sr_2NaNb_5O_{15}$ Bronze

Almudena Torres-Pardo,[†] Ricardo Jiménez,[‡] José M. González-Calbet,[†] and Ester García-González*[,†]

[†]Departamento de Química Inorgánica, Facultad de Químicas, Universidad Complutense Madrid, 28040 Spain

[‡]Instituto de Ciencia de Materiales de Madrid, CSIC Cantoblanco, Madrid, 28049 Spain

Supporting Information

ABSTRACT: An exhaustive temperature dependent structural and dielectric study of the tetragonal tungsten bronze-type $Sr_2NaNb_5O_{15}$ (SNN) compound has been performed in the 300−100 K temperature range, by combining X-ray, neutron diffraction, and transmission electron microscopy with dielectric measurements, in order to clarify the structural effects responsible for the observed low temperature dielectric properties. Interestingly, a relevant second anomaly in the dielectric constant, in addition to the ferroelectric (FE) to paraelectric (PE) transition at T_C = 518 K is found at $T \approx 240$ K, revealing a relaxor-like behavior of the material at low temperature. This phenomenon has been previously observed in FE perovskite-type phases and referred to as the re-entrant phenomenon. However, FE polarization tends to vanish below this low temperature dielectric anomaly and this fact is not expected for a classical relaxor-ferroelectric phase. Although there is no structural transition from RT to 100 K, there is a change in the elastic properties of the material in the considered temperature range and the intense anomaly at ∼240 K could be associated to a smeared-out phase transition to a frustrated FE/ferroelastic (FEL) low temperature state in correlation with subtle structural effects.

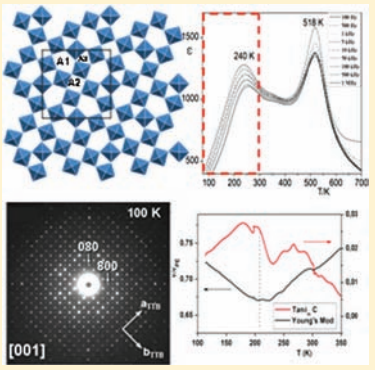

INTRODUCTION

Tetragonal tungsten bronze (TTB)-type ceramics are an exciting class of materials with a huge diversity of properties based on their compositional flexibility. The TTB-type structure can be regarded as a corner sharing MO_3 octahedral framework which creates three different types of cavities, square, pentagonal, and triangular tunnels available for cation inclusion[1] (A1, A2, and A3 sites, respectively, in Figure 1). Various types of stoichiometry are possible depending on the existence of vacancies in A1, A2, or A3 positions. Although the terms "filled" and/or "unfilled" TTBs are often applied in the literature, the small A3 site is empty and the term filled refers to the situation in which A1 and A2 are occupied. The coexistence of different cations favorable in both the octahedral framework as well as in the A sites and the amount of disorder are closely related to the complex dielectric properties of these materials.[2,3] In this sense, TTB niobates constitute an alternative to lead containing piezoelectric ceramics, as is the case of ceramics in the $(1 - x)Sr_2NaNb_5O_{15} - xCa_2NaNb_5O_{15}$ (SCNN) system $(0.05 \leq x \leq 0.35)$.[4,5] Dielectric spectra for these compositions displayed two dielectric anomalies, and it is interesting to note that the low temperature anomaly presents relaxation and shift of the temperature at maximum when increasing the measuring frequency, such behavior resembling the typical Vogel−Fulcher relationship for relaxor ferroelectrics.[6,7] The dielectric characterization of the $Sr_2NaNb_5O_{15}$ composition on both single crystal[8] and dense ceramics[9] have shown similar results: a broad low temperature relaxor-like anomaly is observed in addition to the high temperature maximum around 540 K. Isostructural

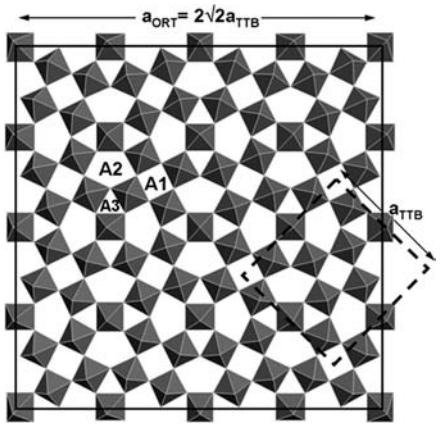

Figure 1. Schematic representation of the structural skeleton of the TTB-type structure projected on the *ab* plane. Square, pentagonal, and triangular tunnels available for cation inclusion are labeled as A1, A2, and A3, correspondingly. The unit cell of both the basic tetragonal substructure as well as the orthorhombic superstructure have been outlined with dotted and solid lines, respectively.

oxides presenting both filled and unfilled structures[10,11] have been extensively studied, showing also this low T anomaly below the FE to PE transition which seems to be insensitive to cation nature and distribution and number of vacancies. Xu et

Received: July 29, 2011
Published: October 28, 2011

   dx.doi.org/10.1021/ic2016098 | *Inorg. Chem.* 2011, 50, 12091−12098

al.[12] associated these anomalies with a phase transition to a monoclinic structure. However, further studies[10] could not find any experimental evidence of this transition which is consistent with the relaxor character observed.

This uncommon behavior has been referred in the literature as the re-entrant phenomenon in perovskite-type materials, and it is explained as associated to a decrease of the long-range interaction of structural dipoles on cooling.[13,14] In the same way that different studies on the isovalent replacement at positions A1 and A2 were used to correlate the structural differences with the displayed ferroelectric properties[15,16] or, more recently, the B-cation effects that have made it possible to correlate quantitative structure−property relations in TTBs,[17] an effort should be made to satisfactorily explain the origin of the low temperature dielectric maximum.

Reentrant relaxor behavior is still a not well-understood phenomenon in perovskite oxides even though the term has been defined for these systems and the structural aspects to be modified for tuning the properties are well-known tools for perovskites. In TTB-type oxides, such phenomenon has not been properly described and also the composition−structure−properties relationship is not well-established. In this sense, the low temperature dielectric properties in TTBs have been tentatively attributed to the inherent randomness of the structure (a vacancies and/or cationic disorder)[10,11,18] or to the concerted rotation of oxygen octahedra,[10,19,20] both giving rise to the vanishing of the macroscopic polarization, but a systematic study that correlates such behavior with a possible structural variation as temperature decreases has not been reported.

Our previous study on polycrystalline SNN describes in detail the structural aspects of the ferroelectric (FE) to paraelectric (PE) phase transition with an emphasis on the structural characterization of the FE room temperature phase in correlation with the dielectric properties.[21] The room temperature phase shows an orthorhombic related TTB structure, space group *Im2a* (no. 46), and cell parameters $a_{ORT} \approx b_{ORT} \approx 2\sqrt{2}a_{TTB}$, $c_{ORT} \approx 2c_{TTB}$ (see Figure 1) with a disordered cationic distribution of Sr and Na atoms in the square (A1) and pentagonal (A2) sites of the TTB skeleton. In addition, the dielectric characterization performed showed the presence of an intense anomaly below room temperature in the temperature dependence of the dielectric constant, as previously stated. Having in mind the fact that the above transition has been already observed in other TTB-type systems and from the lack of satisfactory explanation for this transition in the literature, we found particularly interesting the correlative dielectric and structural study of SNN in the low temperature range, referencing the structure described for the material at room temperature. In this sense, the present study explains the results obtained in the characterization between 300 and 100 K by correlating the structural evolution of $Sr_2NaNb_5O_{15}$ with the observed dielectric properties.

EXPERIMENTAL SECTION

High purity $SrCO_3$ (99,9%, Merck), Na_2CO_3 (99.5%, Merck), and Nb_2O_5 (99.995%, Aldrich) were used for the preparation of polycrystalline $Sr_2NaNb_5O_{15}$ by the conventional ceramic technique. Stoichiometric amounts of the starting materials were mixed in an agate mortar and heated in platinum crucibles at 1173 K for 24 h. The resulting powders were reground in an agate mortar, pelleted, heated in air at 1523 K for two days, and finally quenched to RT.

RT powder XRD patterns were collected on a Panalytical X'PERT PRO ALPHA 1 diffractometer with a Ge(111) primary beam monochromator prealigned for CuKα_1 radiation and provided with a X'Celerator fast detector. Low temperature powder XRD were carried out on a Panalytical X'PERT PRO ALPHA 1 diffractometer with a Ge(111) monochromator and an X'Celerator detector equipped with a TTK450 chamber (Anton Paar) refrigerated with liquid nitrogen. Neutron diffraction was performed using the D2B powder diffractometer at the Institute Laue Langevin (ILL) in Grenoble (France). Experiments were carried out in the temperature range 100−300 K at a wavelength of 0.15405 nm.

Samples for transmission electron microscopy (TEM) were ultrasonically dispersed in *n*-butanol and transferred to carbon coated copper grids. Low-temperature selected-area electron diffraction (SAED) was carried out on a PHILIPS CM20FEG SuperTwin electron microscope by using a liquid nitrogen-cooled specimen holder GATAN 636-DH. Crystal by crystal chemical microanalysis was performed by energy dispersive X-ray spectroscopy (EDXS), carried out on a PHILIPS CM20FEG SuperTwin electron microscope supplied with an EDAX analyzer DX4 (superultrathin window, resolution ≈ 135 eV). From this analysis, crystals showed an Nb:Sr ratio in agreement with the nominal composition. The average cationic composition of the sample, $Sr_{1.97}Na_{1.03}Nb_5O_{15}$, was determined on a JEOL 8900 "Super Probe" Electron Probe Microanalyzer with five wavelength-dispersive X-ray spectrometers (WDS) operating at 20 kV and 50 μA.

Dielectric properties were measured on a precision LCR meter HP 4284A. Measurements were carried out as a function of temperature (80−750 K) at selected frequencies between 10^2 and 10^6 Hz on disk-shaped specimens of 13 mm diameter and 0.9 mm thickness sintered in air at 1373 K for 24 h (density > 95%). Gold paste (Dupont QG 150) sintered at 1123 K was used as an electrode. The polarization electric field (*P*−*E*) hysteresis loops were obtained by means of an in-house made system based on the virtual ground technique. High voltage sine waves of 0.1 Hz frequency were applied by the combination of an HP3325B synthesizer/function generator and a bipolar operational power supply/amplifier (TREK 10/40 A), while charge was measured with an in-house-made charge to voltage converter. The sample was mounted in a Janis VPF 700 to perform the hysteresis loop measurements between 77 and 400 K. The measurement as a function of temperature was performed dynamically with a cooling rate of 1 K·min^{-1}. The sinusoidal perturbing wave was applied to the sample continuously during the whole cooling process. The voltage amplitude was varied during the experiment assuring that the applied field was more than 2.5 times the value of the coercive field at the measuring temperature. The loops were collected at intervals of 10 K.

The low frequency Young's modulus and mechanical losses were measured as a function of temperature by dynamical mechanical analysis in a three-point bending configuration with a Perkin-Elmer DMA 7 apparatus. A stress sine wave of 8.5 MPa was applied to ceramic bars of dimensions 12 × 2 × 0.35 mm^3. Measurements were dynamically accomplished at a single frequency of 9 Hz during cooling from 350 to 100 K at a 2 K·min^{-1} rate. This technique has been shown to be very suitable for studying phase transitions in ferroelectric/ferroelastic phases.[22−24]

RESULTS

Figure 2a shows the temperature dependence of the real part of the relative permittivity (ε_r') at different measuring frequencies for $Sr_2NaNb_5O_{15}$. In addition to the main peak at T_C = 518 K corresponding to the FE−PE transition,[15] a broad maximum around 240 K is observed. A small broad anomaly can also be found at 365 K. The low temperature broad dielectric maximum ε_r' (T_m) is shifted to higher values as frequency increases following the empirical Vogel−Fulcher (V−F) law[25] (inset of Figure 2a), with a freezing temperature T_f = 189 K, activation energy E_a = 160 meV, and relaxation frequency ω_0 close to 1.7 × 10^{18} rad·s^{-1}. The estimation of ω_0 presents large uncertainty due to the limited experimental frequency window,

dx.doi.org/10.1021/ic2016098 | Inorg. Chem. 2011, 50, 12091−12098

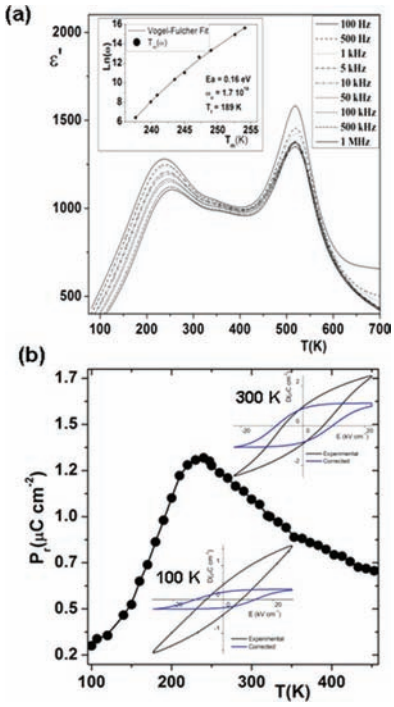

Figure 2. (a) Temperature dependence of ε_r' measured at different frequencies in $Sr_2NaNb_5O_{15}$: (inset) frequency dependence of T_m (points) and Vogel–Fulcher curve corresponding to the maximum located around 240 K. (b) Temperature dependence of the remnant polarization. The values of Pr were obtained from the $P(E)$ hysteresis loops acquired at different temperatures. The insets show the $P(E)$ hysteresis loops recorded for the $Sr_2NaNb_5O_{15}$ material at 300 and 100 K.

but the so large value shows that probably the empirical V–F approach does not correctly describe the present situation. These results indicate the material behaves like a relaxor-ferroelectric material in what refers to the relaxation process of the so-called polar nanoregions.[26,27]

The evolution of the remnant polarization as the temperature decreases is plotted in Figure 2b. As can be observed, it increases on cooling up to 235 K and then it decreases to reach a minimum value at 100 K. It is interesting to note that the temperature at the maximum in the remnant polarization matches with the temperature of the relaxing maximum in ε_r' (Figure 2a). The hysteresis loops measured at selected temperatures have been included as the inset in Figure 2b. After correction of the nonswitching contributions to the loop,[28] the low temperature loops show less saturation polarization than the one obtained for the FE phase at 440 K although retaining rather high coercive field. This FE polarization is not the expected behavior in a relaxor-ferroelectric phase for which field cooling polarization increases or stabilizes.[29] As already mentioned, we emphasize the fact that this phenomenon is observed below the FE–PE transition temperature, and therefore, the loss of the FE character takes place when the temperature decreases. This uncommon behavior, however, has been previously observed in diverse FE TTB-type oxides although its origin has been tentatively explained in different ways.[10,11,18−20] In this sense, we have carried out a systematic temperature dependent structural characterization of $Sr_2NaNb_5O_{15}$ in the $100 \leq T$ (K) ≤ 300 interval by combining selected area electron diffraction, X-ray diffraction, and neutron diffraction.

Figure 3 shows the room temperature XRD pattern for SNN and the sequence of patterns collected as temperature decreases

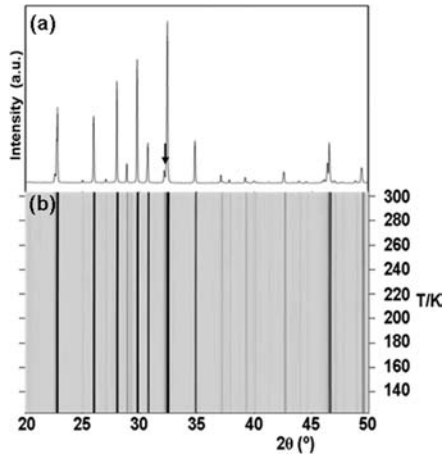

Figure 3. (a) Room temperature XRD pattern for $Sr_2NaNb_5O_{15}$. (b) Temperature-dependent powder XRD data recorded between 303 and 123 K in the isoline plot. The arrow in a shows the most intense reflection of the impurity phase.

from 303–123 K at intervals of 10 K. Neither extra diffraction maxima nor displacements of the existing maxima in the whole temperature interval are observed revealing that no structural transition discernible by X-ray diffraction is associated to the maximum in ε_r' around 240 K in agreement with the relaxor-like character observed.[29] The structural changes related to the disturbance of the interaction of the FE domains must be so marginal that they can hardly be revealed by macroscopic methods. In this sense, we have performed the Rietveld analysis[30] of the neutron diffraction data, very sensitive to oxygen sites investigation, recorded at 100 and 290 K. According to our previous study,[21] atomic positions corresponding to the space group *Im2a* (no. 46 in the $a\bar{c}b$ setting) were used as input data and the sodium and strontium atoms were randomly distributed in the completely filled A1 and A2 sites of the structure. The proposed asymmetric unit cell contains 102 atoms from which 66 are oxygen atoms. Provided the large size of the unit cell as well as the high fraction of light atoms constituting the unit cell, we have performed the structural refinement by using simultaneously the X-ray and the neutron diffraction data recorded at room temperature.

The experimental, calculated, and difference powder X-ray and neutron diffraction profiles of SNN at room temperature are shown in Figure 4a and b, respectively. Table 1 summarizes the corresponding crystallographic parameters. The disordered distribution of strontium and sodium atoms in the A1 and A2 sites of the structure is confirmed from the refined site occupancy factors (crystallographic information file provided as Supporting Information). A minor impurity (about 3%) is observed, which was assigned to the perovskite-type oxide $NaNbO_3$ (JCPDS 01-089-6652), although the presence of a certain amount of strontium in this perovskite-type phase cannot be ruled out provided the existence of $Na_{1-x}Sr_{x/2}NbO_3$ solid solution.[31] The neutron diffraction pattern of $Sr_2NaNb_5O_{15}$ recorded at 100 K is shown in Figure 4c. Neither extra diffraction maxima nor variation in their intensity is observed, allowing us to consider the room temperature structure model as input data for the refinement of the low temperature data. The structural and crystallographic parame-

dx.doi.org/10.1021/ic2016098 | *Inorg. Chem.* 2011, 50, 12091–12098

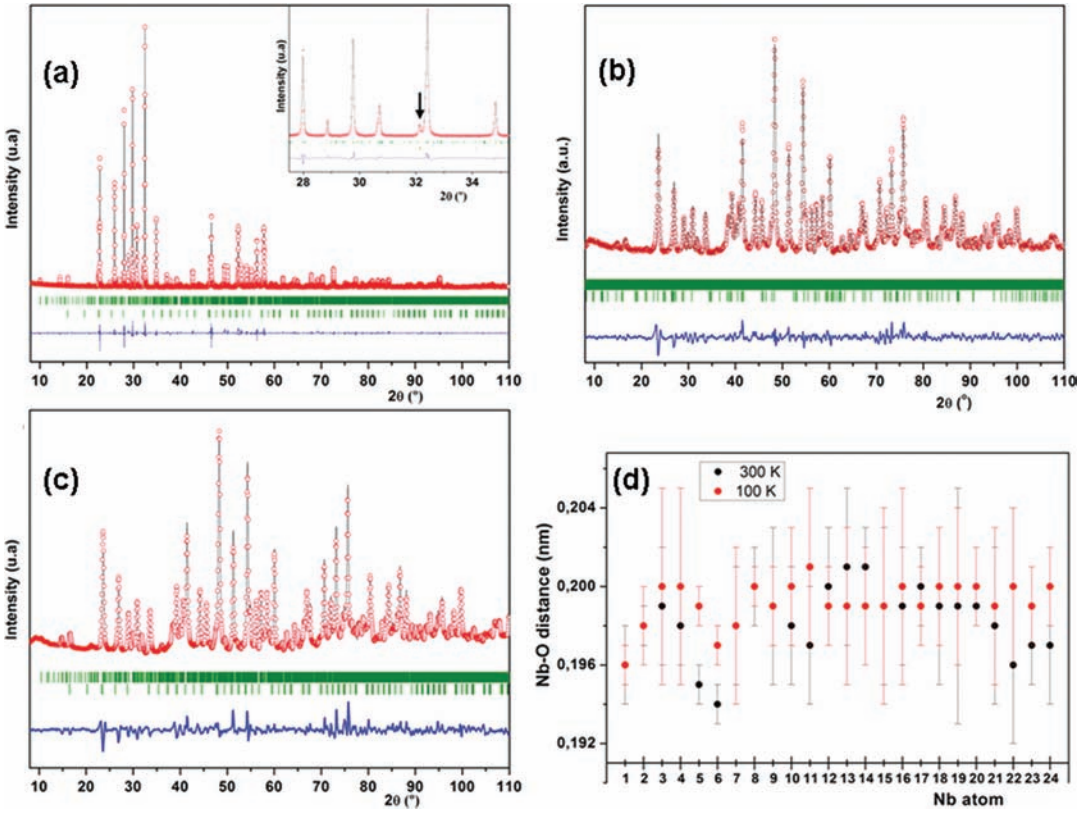

Figure 4. Experimental, calculated, and difference profiles obtained from the Rietveld refinement of (a) room temperature powder XRD pattern, (b) room temperature powder ND pattern, and (c) powder ND pattern at 100 K on $Sr_2NaNb_5O_{15}$. (d) Averaged (Nb−O) distances obtained from the structural refinement at 100 and 300 K.

Table 1. Crystallographic Data for $Sr_2NaNb_5O_{15}$ at 300 and 100 K

temperature	300 K		100 K
space group	*Im2a* (no. 46)		*Im2a* (no. 46)
a (Å)	34.996(3)		34.989(3)
b (Å)	34.934(3)		34.891(3)
c (Å)	7.789(5)		7.791(1)
B A1sites (nm)	0.08		0.046
B A2 sites (nm)	0.13		0.046
pattern	XRD	ND	ND
R_p	8.73	4.84	3.94
R_{wp}	12.1	6.18	5.14
R_{exp}	6.03	1.62	1.51
R_B	5.07	5.68	5.18
χ^2	4.03	14.5	11.6

ters obtained from the corresponding Rietveld refinement are summarized in Table 1, and the corresponding crystallographic information file is provided as Supporting Information.

Comparison of the Nb−O and Sr/Na−O average distances at 100 and 300 K (Figure 4d) does not show significant differences, thus leading one to consider that no structural variation takes place between the two temperatures. A significant evolution occurs, however, in the thermal factor of strontium and sodium atoms by decreasing the temperature, as revealed by the neutron diffraction study. In this sense, the room temperature value of the isotropic thermal factor (B) for strontium and sodium atoms in the pentagonal A2 sites (0.13 nm) is clearly higher than the value obtained in the perovskite-type A1 sites (0.08 nm). This fact reflects the delocalization of the relatively small sodium and strontium atoms in the larger pentagonal sites. As expected, the isotropic thermal factors decrease by decreasing the temperature, but it is worth mentioning that those corresponding to Sr/Na cations located in the A1 and A2 cavities tend to equalize both reaching a value of 0.046 nm.

The stabilization of an incommensurate phase of the TTB-type structure has been proposed as the origin of the relaxor-type behavior observed below T_C in the case of the $(Sr_{0.61}Ba_{0.39})_5Nb_{10}O_{30}$ material.[10] In this sense, we have followed the structural evolution of $Sr_2NaNb_5O_{15}$ by recording SAED patterns at 300 and 100 K. Figures 5a−f show the SAED patterns of the SNN along the [001], [100], and $[10\bar{1}]$ zone axes recorded at 293 and 100 K. As observed, there are no differences between the diagrams at low temperature and those recorded at room temperature. The SAED patterns along the [001] zone axis are shown in Figures 5a and b. Besides the main reflections of the TTB substructure, a weaker diffraction maxima located at $(h/2\ k/2\ 0)_{TTB}$ indicates an orthorhombic distortion of the TTB basic unit cell. By tilting around the orthorhombic axis, corresponding SAED patterns along $[100]_{ORT}$ and $[10\bar{1}]_{ORT}$ zone axes (Figures 5c and d and e and f, respectively) are obtained, showing extra diffraction maxima located at $(0\ k/2\ l/2)$ and $(h/2\ k\ l/2)$, respectively. These results confirm that the room temperature orthorhombic superstructure $2\sqrt{2}a_{TTB} \times 2\sqrt{2}a_{TTB} \times 2c_{TTB}$ remains below the low temperature dielectric maximum T_m = 240 K.

The anomalous variation of the unit cell volume with temperature is a distinctive trait of relaxor-like materials,[27] and it is also observed in SNN. Figure 6a shows the loss of the linear variation around 280 K which agrees with the relaxor-like

dx.doi.org/10.1021/ic2016098 | *Inorg. Chem.* 2011, 50, 12091−12098

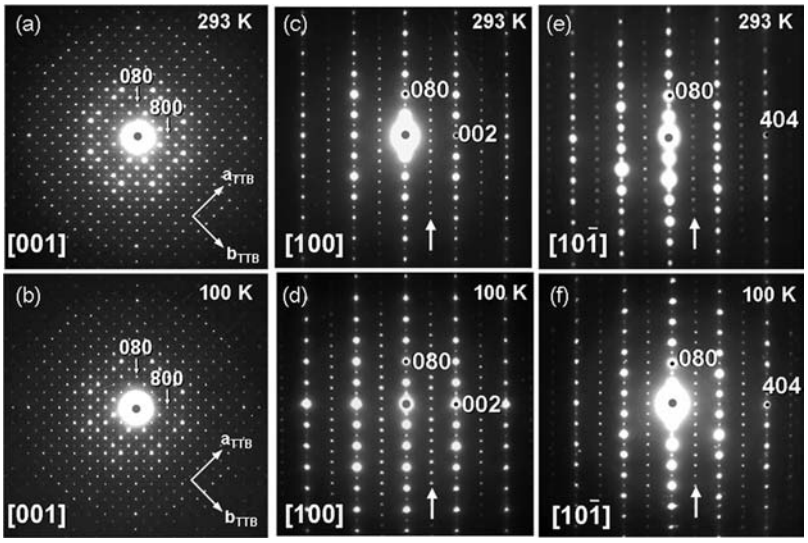

Figure 5. SAED patterns of $Sr_2NaNb_5O_{15}$ taken along (a and b) $[001]_{ORT}$, (c and d) $[100]_{ORT}$, and (e and f) $[10\bar{1}]_{ORT}$ zone axes recorded at 293 and 100 K. The arrows indicate the (0 k/2 l/2) and (h/2 k l/2) reflections for the $[100]_{ORT}$ and $[10\bar{1}]_{ORT}$ zone axis, respectively.

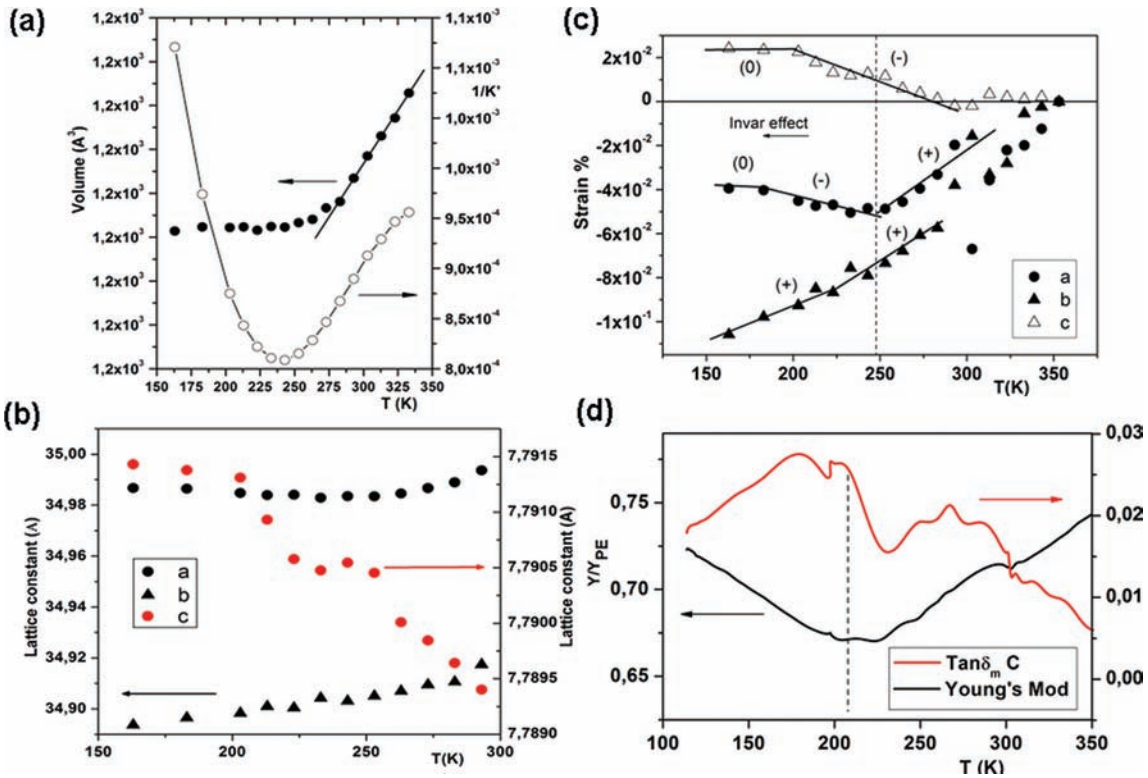

Figure 6. (a) Temperature dependence of the volume of the unit cell and $1/K'$ for $Sr_2NaNb_5O_{15}$. (b) Evolution of the lattice parameters from 300 to 100 K obtained from the XRD diagrams. (c) Temperature evolution of the strain of the orthorhombic cell parameters. Brackets show the sign of the thermal expansion coefficients. Straight lines point out the regions with different thermal expansion behavior. The dashed line indicates the beginning of the invar effect. (d) Temperature evolution of the Young's modulus and the mechanical loss tangent as a function of temperature on cooling. The Young's modulus values are normalized with the value of the high temperature PE phase. The dashed line indicates the freezing temperature obtained from the dielectric measurements.

character observed at low temperature. The anisotropic variation of the evolution of the cell parameters in the 100–300 K temperature range is shown in Figure 6b. As can be observed, the b lattice parameter decreases with cooling while the a lattice parameter decreases until 250 K and then remains constant up to around 150 K where it starts a small rise. On the other hand, the value of the c lattice parameter increases up to 200 K where it tends to stabilize, although a small anomaly around 250 K can be identified.

From the evolution of the lattice parameters, the strain associated to each of them can be calculated by using the lattice constant measured at 350 K as a reference. Figure 6c reveals a complex thermal expansion behavior. As can be observed, the a lattice parameter changes from positive thermal expansion

dx.doi.org/10.1021/ic2016098 | Inorg. Chem. 2011, 50, 12091–12098

coefficient to negative around 250 K while the *c* parameter presents negative thermal expansion coefficient from 300 to 200 K, showing then almost zero value. In the case of the *b* lattice parameter, a positive thermal expansion coefficient in the whole temperature range is observed, showing a reduction of the coefficient for temperatures below 250 K.

DISCUSSION

The electrical characterization performed on $Sr_2NaNb_5O_{15}$ reveals the material losses his ferroelectric character on cooling from 300 K, showing dynamic relaxor-like character below the ferroelectric−paraelectric transition which suggests a re-entrant behavior for this material. As mentioned, this unusual phenomenon has been previously observed in other TTB-type ferroelectric materials, but the term re-entrant has only been used in the literature as referred to perovskite-type materials.[13,14] From these studies, the breakdown of the long-range ferroelectric state should occur as a result of the presence of disordered polar regions of nanometer size, the so-called polar nanoregions (PNRs), within the ferroelectric phase, but it is a not well-understood phenomenon.

Previous measurements on the dielectric behavior with temperature of the TTB-like $Sr_{1.9}Ca_{0.1}NaNb_5O_{15}$ single crystals showed polydispersivity and relaxation in the low temperature anomaly when measuring the dielectric response along the [110] direction.[7] In this crystalline direction, no anomalies associated to the FE−PE phase transition appeared which, however, were observed along the uniaxial [001] direction. The reported explanation for this low temperature anomaly is a freeze-out of the dielectric polarizability effects rather than a phase transition. It should be noticed that in SNN single crystals a small low temperature anomaly can also be found along [001], indicating some effects on the polarizabity.[8] In random ceramic samples without any texture, as is the case of the samples in the present work, the dielectric response is a weighted average of the dielectric tensors and so all the anomalies should be present. If the low temperature anomaly is present in the [100] and [010] directions, it will be enhanced in the averaged response in comparison with the higher temperatures anomalies that are present along the [001] direction. The observed dielectric behavior in the SNN ceramic corresponds to this situation.

As it has been stated,[32] the appearance of PNRs and their growth must be related to the correlation and distribution of quenched random fields (RF) that came from charge disorder present in the material. The presence of the PNRs occurs when the thermal fluctuations are slow enough to allow the influence of the statistical fluctuations of the RFs to act and then grow up when lowering the temperature.

In the case of the SNN oxide, the observed disordered occupation of A1 and A2 sites by Sr and Na can provide the chemical and charge disorder in the same crystallographic position that would enable the formation of PNRs in the material and, consequently, its interaction when decreasing temperature.[29] The small ionic size differences between Sr^{2+XII} (1.44 Å) and Na^{+XII} (1.39 Å) can justify the observed disorder. On the other hand, when Sr is substituded by Ca, the smaller Ca^{2+} (1.34 Å) ion tends to occupy the A1 site. The reduced disorder produces a decrease on the diffusivity and poly-dispersitivity of the low temperature anomaly although keeping its relaxor character.[4] However, the decrease of the remnant polarization on cooling (see Figure 2b) as well as the remarkably high value of the dielectric constant (see Figure 2a) associated to the relaxor character at low temperature, make a difference with the relaxor-like behavior of SNN from that previously observed in perovskite type systems, where P_r remains constant for temperatures below the freezing temperature.[13,14] In addition, the loss of long-range interaction is opposite to the phenomena observed in classical relaxor-type materials, the long-range interactions increasing on cooling down to the freezing temperature which in some cases produces a stable FE state in the material.[26,29,33] The loss of both remnant and saturation polarization on cooling that we observed for the SNN compound indicates that the PNRs produced are not able to grow and to create a stable polarization and that the saturation polarization related to the new phase is low, interfering with the FE polarization of the host matrix. Therefore, a structural study performed could shed some light in trying to find the possible origin of such an electrical behavior.

From the characterization carried out by SAED as a function of temperature, it seems that the relaxor-like behavior of the SNN material is not correlated to the loss of long-range order in the octahedral skeleton as it was previously reported for $(Sr_{0.61}Ba_{0.39})_5Nb_{10}O_{30}$.[10] In this case, the concerted rotation of NbO_6 octahedra stabilizes an incommensurate phase which could induce a weak variation of the dipolar moments at the unit cell level thereby altering the macroscopic dielectric response of the material. However, it is important to note that the structural characterization of the material is performed in the temperature range 93−493 K and, therefore, failure to provide information about possible structural variations around and below the temperature of the dispersive maximum observed ∼60 K. In the case of the SNN material, the structural study by transmission electron microscopy clearly shows that incommensurate phases are neither present nor stabilized with decreasing temperature which leads us to look for a different origin of the relaxor-like behavior at low temperature.

Although the characterization performed indicates that no structural transition occurs below T_m = 240 K, the loss of polarization must indeed originate from slight displacements of atoms which introduce a disturbance in their interaction in the ferroelectric phase. From the analysis of the neutron diffraction data, the value of the thermal parameters of cations located in the tunnels of the skeleton of the TTB structure drops from RT to 100 K, thermal factors of Sr and Na cations showing a clear trend to equalize up to 0.046. The expected decrease in the isotropic thermal parameter as a result of the decreasing temperature seems to be related to the trend of those atoms to be localized in their positions within the pentagonal cavities as opposite to the relative delocalization experimented at room temperature. The slight local structural changes could result in small local variations of the dipoles which modify their long-range interaction, changing the degree of polarization at the unit cell level and giving rise to the dispersive-relaxor character observed in the dielectric permittivity. This is also consistent with the observed loss of the remnant polarization on cooling if as commented before the polarization of the PNRs is much lower than the FE polarization of the FE matrix.

At this point, it is important to mention that the relaxor-type character of SNN as well as in all the previously investigated TTBs[10] is identified with a well-defined low temperature maximum in the $\varepsilon_r'-T$ curve as opposite to the observed for the perovskite-type solid solution with re-entrant behavior studied by Lei et al.[14] In that case, the relaxor character is seen as a

small low temperature anomaly whose maximum intensity of ε_r' is clearly lower than the value of the high temperature FE−PE transition. This fact suggests that relaxor behavior of this material occurs in a limited portion of the volume differing with the bronze compound, where the relaxor-like behavior must occur in the entire volume of the material.

From the analysis of the temperature evolution of the thermal expansion coefficients, information about the polarization direction can be obtained. It should be borne in mind that negative values of the thermal expansion coefficient are usually found in the polar axis of FE materials.[34] In this sense, the change in the sign of the thermal expansion coefficient of the *a* lattice parameter can be related to a subtle rotation of the polarization toward the *a* axis when lowering the temperature. The rotation of the polarization vector from the [001] direction toward [110] was already proposed to explain the low temperature dielectric peak in some ferroelectric niobate crystals with TTB-type structure changing the symmetry from orthorhombic to monoclinic.[12] However, the observed FE polarization values of the low and high temperature phases are similar, which is not the behavior we have found for the SNN compound.

On the other hand, the invar effect observed for the SNN compound presents a different origin to that found in model relaxors like lead metaniobate $PbMn_{1/3}Nb_{2/3}O_3$.[26,29] For materials with orthorhombic symmetry like SNN, the three different cell axes should be compensated to produce the invar effect in the cell volume whereas in relaxor materials with cubic symmetry, the invar volume effect matches with the vanishing of the thermal expansion of the cubic axis. The emergence of the invar effect coming from the ferroelectric orthorhombic phase can be related to a change in the strain of the cell. In that case, the appearance of strain in the unit cell of SNN below 300 K (see Figure 6c) could be associated to a smeared phase transition to a frustrated FE/FEL low temperature state that should provoke an effect (minimum) in the Young's modulus of the material.

In relaxor-type materials like PMN, the Young's modulus as a function of T presents a minimum close to the T_m of the dielectric anomaly and a kink coupled with a maximum in the mechanical loss at temperature close to the freezing one.[35,36] Figure 6d shows the evolution of the complex Young's modulus of SNN in the interval 100−350 K. A broad minimum around 230 K as well as a maximum close to the freezing temperature are observed in the mechanical losses, indicating a change of the elastic properties of the material in the considered temperature range. Assuming that at 300 K the SNN is FE and FEL,[8] the loss of long-range FE interactions can be related to the presence of a smeared out phase transition to a frustrated FE/FEL low temperature state that produces a continuous change in the TTB-crystalline cell dimensions at constant volume producing strain and a subtle rotation of the polar axis that could be correlated with the stabilization of the Sr/Na cations in the pentagonal sites of the structure without any apparent change of the macroscopic crystal symmetry. Therefore, the re-entrant behavior observed in the SNN compound presents features related to the onset of a relaxor-like state, but the behavior of the ferroelectric polarization on field cooling does not support a conventional character. Rather it appears that the onset of the PNRs produced the vanishing of the FE polarization due to the breaking of the long distance correlation in the FE domains and reducing the FE volume in the sample. On decreasing the temperature, the volume of PNRs increases and so the FE polarization vanishes when the FE percolative cluster breaks and the relaxor-like phase dominates. The coexistence of a cluster glass with an antiferromagnetic phase has been recently found in multiferroic $PbFe_{0.5}Nb_{0.5}O_3$,[37] so the coexistence of a relaxor-like state in a FE matrix seems to be supported. In this sense, we cannot rule out a change of the local symmetry of the crystalline region inside the PNRs as proposed by Xu et al.[12] In that case, the TTB can change from uniaxial ferroelectric to a different situation but with smaller saturation polarization than the parent FE phase, as the remnant polarization value at 100 K indicates (see Figure 2b).

In summary, the relevant second anomaly observed in the dielectric constant in ceramics of SNN at $T_m \approx 240$ K reveals relaxor-like character for the material at low temperature. The loss of the FE character takes place when temperature decreases although such loss of long-range interaction is opposite to the phenomenon observed in classical relaxor-type materials. The structural characterization performed indicates that no transition seems to occur from RT to 100 K preserving the orthorhombic superlattice $2\sqrt{2}a_{TTB} \times 2\sqrt{2}a_{TTB} \times 2c_{TTB}$. However, the strain observed in the orthorhombic cell as well as the localization of the Na and Sr atoms in the A2 pentagonal sites on cooling can indicate the occurrence of a smeared phase transition to a frustrated FE/FEL state that could involve the rotation of the polar axis. The appearance of the low temperature PNRs reduces the volume of the FE parent phase on decreasing the temperature producing the observed vanishing of the FE polarization. From the results obtained, the re-entrant behavior observed in this TTB structure cannot be simply correlated with the onset of a "classical" relaxor state. These results point out in the same direction as the tentative explanations given before by other authors for different compositions. Randomness of the structure is intrinsic to most TTBs: they are often unfilled and/or disordered in cation distribution and different environments occur from site to site in the crystals. Then, polarization fluctuations take place driven by these small structural changes in the channels of the TTB structure.

■ ASSOCIATED CONTENT

Supporting Information

Crystallographic data in CIF format for $Sr_2NaNb_5O_{15}$ at 300 and 100 K. This material is available free of charge via the Internet at http://pubs.acs.org.

■ AUTHOR INFORMATION

Corresponding Author

*Tel.: +34-913944518. Fax: +34-913944352. E-mail: esterg@quim.ucm.es.

■ ACKNOWLEDGMENTS

Financial support from DGICYT in Spain through Projects MAT2007-61954 and MAT2007-61409 is gratefully acknowledged. Authors are grateful to the Centro de Difracción de Rayos X (U.C.M.) and to the Centro de Microscopia Electrónica Luis Bru (U.C.M.) for facilities and to Dr. Juan Rodríguez Carvajal for helpful assistance and fruitful discussions.

■ REFERENCES

(1) Hyde, G.; O'Keefe, M. *Acta Crystallogr.* **1973**, *A29*, 243.

(2) Simon, A.; Ravez, J. *C. R. Chim.* **2006**, *9*, 1268.
(3) Hornebecq, V.; Elissalde, C.; Weill, F.; Villesuzanne, A.; Menetrier, M.; Ravez, J *J. Appl. Crystallogr.* **2000**, *33*, 1037.
(4) Xie, R. J.; Akimune, Y. *J. Mater. Chem* **2002**, *12*, 3156−3161.
(5) Xie, R. J.; Akimune, Y.; Wang, R. P.; Hirosaki, N. J. *Am. Ceram. Soc.* **2002**, *85* (11), 2731−2737.
(6) Torres-Pardo, A.; Jiménez, R.; González-Calbet, J. M.; García-González, E. *Chem. Mater.* **2009**, *21*, 2193.
(7) Neurgaonkar, R. R.; Cory, W. K.; Oliver, J.; Sharp, E. J.; Wood, G. L.; Miller, M. J.; Clark, W. W.; Salamo, G. J. *Mater. Res. Bull.* **1988**, *13*, 1459.
(8) Van Uitert, L. G.; Levinstein, H. J.; Rubin, J. J.; Capio, C. D.; Dearborn, E. F.; Bonner, W. A. *Mater. Res. Bull.* **1968**, *3*, 47.
(9) Kimura, M.; Manimakawa, T.; Ando, A; Skabe, Y. *Jpn. J. Appl. Phys.* **1997**, *36*, 6051.
(10) Ko, J.-H.; Kojima, S.; Lushnikov, S. G.; Katiyar, R. S.; Kim, T.-H.; Ro, J.-H. *J. Appl. Phys.* **2002**, *92*, 1536.
(11) Levin, I.; Stennet, M. C.; Milles, G. C.; Woodward, D. I.; West, A. R.; Reaney, I. M. *Appl. Phys. Lett.* **2006**, *89*, 122908.
(12) Xu, Y.; Li, Z.; Wang, W. LiH.; Chen, H. *Phys. Rev.B* **1989**, *40*, 11902.
(13) Yan Guo, H.; Lei, Ch.; Ye, Z. G. *Appl. Phys. Lett.* **2008**, *92*, 172901.
(14) Lei, Ch; Ye., Z. G. *J. Phys.: Condens. Matter* **2008**, *20*, 232201.
(15) Miles, G. C.; Stennett, M. C.; Reaney, I. M.; West, A. R. *J. Mater. Chem.* **2005**, *15*, 798.
(16) Stennett, M. C.; Miles, G. C.; Sharman, J.; Reaney, I. M.; West, A. R. *J. Eur. Ceram. Soc.* **2005**, *25*, 2471.
(17) Arnold, D. C.; Morrison, F. D. *J. Mat. Chem.* **2009**, *19*, 6485.
(18) Simon, A.; Ravez, J.; Maglione, M. *Solid State Sci.* **2005**, *7*, 92.
(19) Bursill, L. A.; Lin, P. J. *Acta Crystallogr. B* **1987**, *43*, 49.
(20) Amorín, H.; Pérez, J.; Fundora, A.; Portelles, J.; Guerrero, F.; Soares, M. R; Martínez, E.; Sequeiros, J. M. *Appl. Phys. Lett.* **2003**, *83*, 4390.
(21) García-González, E.; Torres-Pardo, A.; Jiménez, R.; González-Calbet, J. M. *Chem. Mater.* **2007**, *19*, 3575.
(22) Kityk, A. V.; Schranz, W.; Sondergeld, P.; Salje, E. K. H.; Scott, J. F. *Phys. Rev. B* **2000**, *61*, 946.
(23) Jiménez, B.; Jiménez., R. *Phys. Rev. B* **2002**, *66*, 014104.
(24) Jiménez, R.; Castro, A.; Jiménez, B. *Appl. Phys. Lett.* **2003**, *83*, 3350.
(25) Viehland, D.; Jang, S. G.; Cross, L. E.; Wutting, M. *J. Appl. Phys.* **1990**, *68*, 2916.
(26) Cross, L. E. *Ferroelectrics* **1987**, *76*, 241−267.
(27) Bokov, A. A.; Ye, Z.-G. *J. Mater. Sci.* **2006**, *41*, 31−52.
(28) Jimenez, R.; Alemany, C.; Calzada, M. L.; Gonzalez, A.; Ricote, J.; Mendiola, J. *Appl. Phys. A−Mater. Sci. Process.* **2002**, *75* (5), 607−615.
(29) Samara, G. A. *J. Phys.: Condens. Mater* **2003**, *15*, R367−R411.
(30) Rodríguez-Carvajal, J.; Roisnel, T. FullProf, WinPLOTR and accompanying programs at http://www-llb.cea.fr/fullweb/powder.htmf, 1999 (accessed February 2007).
(31) Torres-Pardo, A.; Jiménez, R.; González-Calbet, J. M.; García-González, E. *Chem. Mater.* **2008**, *20*, 6957.
(32) Kleemann, W. J. *Mater. Sci.* **2006**, *41*, 129.
(33) Cowley, R. A.; Gvasaliya, S. N.; Lushnikov, S. G.; Roessli, B.; Rotaru, G. M. *Advan. Phys.* **2011**, *60*, 229.
(34) Krishnan, R. S.; Srinivasan, R.; Devanarayanan, S. *Thermal expansion of crystals*. International Series in the Science of the Solid State; Pergamon Press Ltd.: Oxford, England, 1979; Vol. *12*.
(35) Yang, F; Bao, P; Wang, Y. *Appl. Phys. Lett.* **2003**, *83* (21), 4384.
(36) Jiménez, R; Jiménez, B; Carreaud, J.; Kiat, J. M.; Dkhil, B; Holc, J.; Kosec, M.; Alguero, M. *Phys. Rev. B* **2006**, *74*, 184106.
(37) Kleemann, W; Shvartsman, V. V.; Borisov, P. *Phys. Rev. Lett.* **2010**, *105*, 257202.